Mobility percolation as a source of Johari-Goldstein relaxation in glasses

Liang Gao,[1] Yang Sun [ORCID],[2] and Hai-Bin Yu [ORCID][1,*]

[1]*Wuhan National High Magnetic Field Center and School of Physics, Huazhong University of Science and Technology, Wuhan 430074, Hubei, China*

[2]*Department of Physics, Xiamen University, Xiamen, Fujian 361005, China*

The Johari-Goldstein secondary (β) relaxations are intrinsic features of supercooled liquids and glasses, and they play a crucial role in several properties of glassy materials. However, their structural origin remains elusive. Prevailing theories consider them as localized activation or "islands of mobility." In this study, we utilize atomistic simulations and percolation analysis to demonstrate that the mobile clusters are actually percolated at the occurrence of β relaxation, in seven different glassy systems. The percolation transition shows the same temperature and time dependence with β relaxation. Percolation emerges universally when about 10% of the atoms are mobile, and the dimension of the system-spanning cluster is approximately 2. Our findings add an essential piece to the full picture for the understanding of β relaxation in glasses.

I. INTRODUCTION

Disordered systems such as glasses and supercooled liquids exhibit a wealth of dynamic processes, known as relaxations [1–7]. They have a significant impact on the mechanical and functional properties of glassy materials [8–12]. They have also been used as probes to interrogate the structure-property relation in disordered systems [13–21]. It is crucial to comprehend how structural rearrangements govern the relaxation processes in order to reveal the nature of glass and design amorphous materials with enhanced properties [22–26].

One particular relaxation, known as the Johari-Goldstein (or secondary or β) relaxation, has garnered significant attention in recent decades [27–33]. It has been observed in a wide range of glassy materials including molecular, oligomeric, polymeric, ionic, metallic, and chalcogenide glasses, among others [20,34–38]. It is usually the dominant relaxation in glass states. Moreover, it has been discovered that several properties of glasses are correlated with β relaxations. For instance, the mechanical properties of metallic and polymeric glasses [39–41], the crystallization speed of phase-change materials [42], and the stability of glassy medicines [43] have all been found to be correlated with β relaxations.

Meanwhile, accumulating evidence indicates the important role of β relaxation from the glass theory perspective. Several studies have shown that the kinetics of liquid-glass transition are not solely driven by the primary structural relaxation, as conventionally believed. Instead, the β relaxation must also have a role in decreasing the activation energy barrier and aiding atomic dynamics in order to facilitate the transition kinetics [44–47].

Despite its technological relevance and theoretical significance, the structural rearrangements governing the β relaxations are still not clearly established. Therefore, the correlations between different properties and β relaxation remain unclear. At present, most of the prevailing models consider that the β relaxation is due to localized events. For example, Johari proposed a picture of the "islands of mobility" where the glass structure is relatively loose and molecules move fast [48,49]. In a recent entropy analysis, he pointed out that the β relaxation likely occurs in local equilibrium regions in a glass structure [50].

Harmon *et al.* suggested that the β relaxation corresponds to the activation of isolated shear transformations, which are confined within the elastic matrix [51]. Liu *et al.* suggested that the β relaxation originates local cooperative bonding switch between the two nearest neighboring large solvent atoms [19]. Wang *et al.* reported that the β relaxation in two La-based metallic glasses mainly depends on the vibration of small Ni and Cu atoms in local cages [52]. On the other hand, from a potential energy landscape perspective, the β transitions have also been considered as the stochastically activated hopping events across "sub-basins" confined within the inherent "mega-basins" [15,53].

In this work, we critically examine whether or not the motions of mobile clusters are localized at β relaxation. This is of key importance for revealing the origin of the β relaxation in glassy materials. We illustrate in seven different glass systems ($Al_{90}Sm_{10}$, $Al_{85}Sm_{15}$, $Ni_{80}P_{20}$, $Cu_{50}Zr_{50}$, $Cu_{65}Zr_{35}$, $Pd_{80}Si_{20}$, and SiO_2) that the mobile clusters are actually percolated at the occurrence of β relaxation.

The percolation transitions could serve as a microscopic signature for the β relaxation as they show the same temperature and time dependence. Our results also suggest that the early or late percolation of mobile clusters has a direct consequence on behaviors of β relaxation and excess wing.

II. RESULTS

As the first typical example, shown in Fig. 1(a), we investigate the complex relaxation dynamics of the $Al_{90}Sm_{10}$

*haibinyu@hust.edu.cn

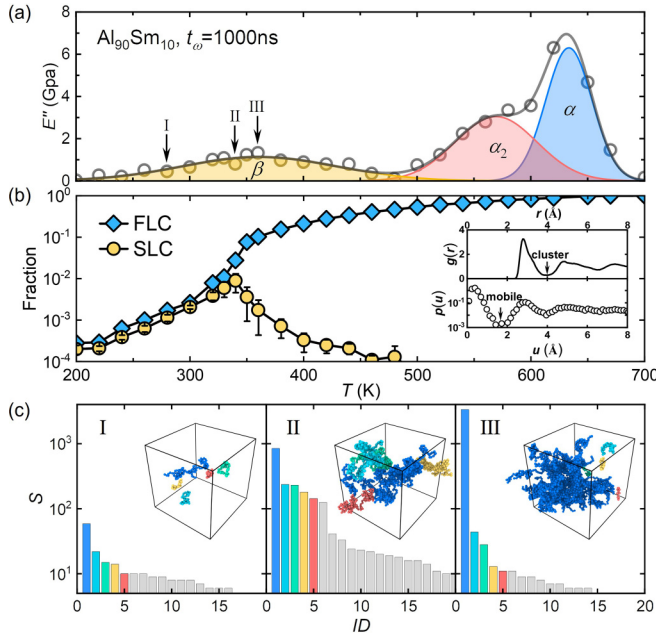FIG. 1. Relaxation and percolation of $Al_{90}Sm_{10}$ model glass. (a) Loss modulus (E'') of the $Al_{90}Sm_{10}$ model system with an oscillation period $t_\omega = 1000$ ns. (b) Fraction of number of atoms for the first-largest (FLC, blue) and second-largest (SLC, yellow) clusters as a function of temperature. (c) The size S (number of atoms for a cluster) of top 20 clusters at $T= 280, 340,$ and 360 K, labeled I, II, and III, respectively. The insets are the top five clusters.

model metallic glass (MG) by molecular dynamic simulations of dynamic mechanical spectroscopy (MD-DMS; Fig. S1 and method in Supplemental Material [54], which contains Refs. [55–66]), which implements the experimental DMS protocols in MD simulations [62,67].

The loss modulus (E'') as a function of temperature exhibits three distinct peaks which are due to the α, α_2, and β relaxations, respectively. Previous studies have clarified that the α_2 relaxation corresponds to the decoupled most probable motions of Al and Sm atoms, while the β relaxation is correlated with the stringlike cooperative atomic relaxation [20].

Following the method of Ghosh and co-workers [68], we calculate the fraction of the first-largest cluster (FLC) and the second-largest cluster (SLC) as a function of temperature. Here, the mobile atoms are defined as those with atomic displacements larger than 1.8 Å, corresponding to the first minimum of the displacement distribution function $p(u)$. Mobile atoms with spatial distance less than 4 Å are considered as in the same cluster. This threshold value is based on the first minimum of the radial distribution function $g(r)$. The mobile and cluster cutoff values for all glassy systems are presented in Fig. S2 and Table S1 of the Supplemental Material [54]. The time period used for the mobile cluster analysis is the same as the oscillation period in the MD-DMS simulation.

Figure 1(b) shows that FLC and SLC exhibit different evolution as the temperature increases. While they both increase initially with temperature, the FLC takes over at $T_{SLC} = 340$ K and saturates at a temperature above $T_\alpha = 635$ K. The SLC stops growing and decays at $T_{SLC} = 340$ K, and vanishes at

$T = 500$ K. This implies that the FLC starts to dominate the system at the expense of SLC and other clusters, which is a signature of the percolation of the FLC.

Comparing Figs. 1(a) and 1(b), one can see that the percolation of the FLC occurs at nearly the same temperature as the β relaxation peak. To understand the evolution of the FLC, we plot the size of the top 20 clusters at $T = 280, 340,$ and 360 K in Fig. 1(c), corresponding to the labels I, II, and III in the MD-DMS curve in Fig. 1(a), respectively.

From I to II, with increasing temperature, these clusters grow in size, and new clusters appear in the configuration space. From II to III, the growth of FLC starts to be accompanied by the reduction of populations in other clusters. This indicates that FLC achieves growth by merging adjacent clusters, which is shown in the insets of Fig. 1(c). Eventually, FLC occupies the entire space. This process is a manifestation of the percolation of FLC. In addition, we demonstrate the similar cluster evolution in other MG systems, as depicted in Fig. S3 [54].

We further examine the correlation between the FLC percolation and β relaxation in other models of MGs at different observation times t_ω. In Fig. 2, we plot the evolution of loss modulus and cluster fractions for three MG systems at different oscillation periods t_ω, $Al_{90}Sm_{10}$ (the left column), $Ni_{80}P_{20}$ (the middle column), and $Cu_{50}Zr_{50}$ (the right column) model MGs.

These three MG systems represent typical behaviors of β relaxation. $Al_{90}Sm_{10}$ exhibits a separated peak; $Ni_{80}P_{20}$ exhibits β relaxation as pronounced humps due to partial overlap with the α relaxation. In $Cu_{50}Zr_{50}$, the β relaxation is not obvious, but there is still an excess contribution to the low-temperature side of the α relaxation, which is known as the excess wing.

We find that these MG systems all exhibit the same correlation as that in Fig. 1. In the case of the $Al_{90}Sm_{10}$ and $Ni_{80}P_{20}$ models, the β relaxation peak and percolation of the FLC shift towards higher temperatures as t_ω decreases, indicating that these are dynamic processes. Both the β relaxation peak and percolation of the FLC depend on the temperature and the observation time. Generally, higher temperature corresponds to shorter relaxation time.

Even in the $Cu_{50}Zr_{50}$ system where excess wings make the determination of β relaxation less precise compared to $Al_{90}Sm_{10}$ or $Ni_{80}P_{20}$, we can still identify that the percolation of FLC happens in the same temperature range where deviations of E'' from the tails of α relaxation are noticeable. These systems with other oscillation periods are shown in Figs. S4–S6 [54]. Similar observations have also been found in $Al_{85}Sm_{15}$, $Pd_{80}Si_{20}$, $Cu_{65}Zr_{35}$, and SiO_2 glassy systems, as shown in Figs. S7–S9.

We evaluated the radius of gyration $R_g = \sqrt{1/2[\sum_{ij}(r_i - r_j)^2/S^2]}$ [69] as a function of the size of mobile cluster S for glassy models with different compositions, oscillation periods t_ω, and temperature, before and near the percolation transition. As shown in Figs. 3(a) and 3(b), these data can be collapsed on a single master curve and be fitted by a scaling relation $R_g \propto S^{1/d_f}$, with the dimension $d_f \approx 2$. This universal scaling indicates that the mobile clusters are fractal, fluffy, and not compact, which
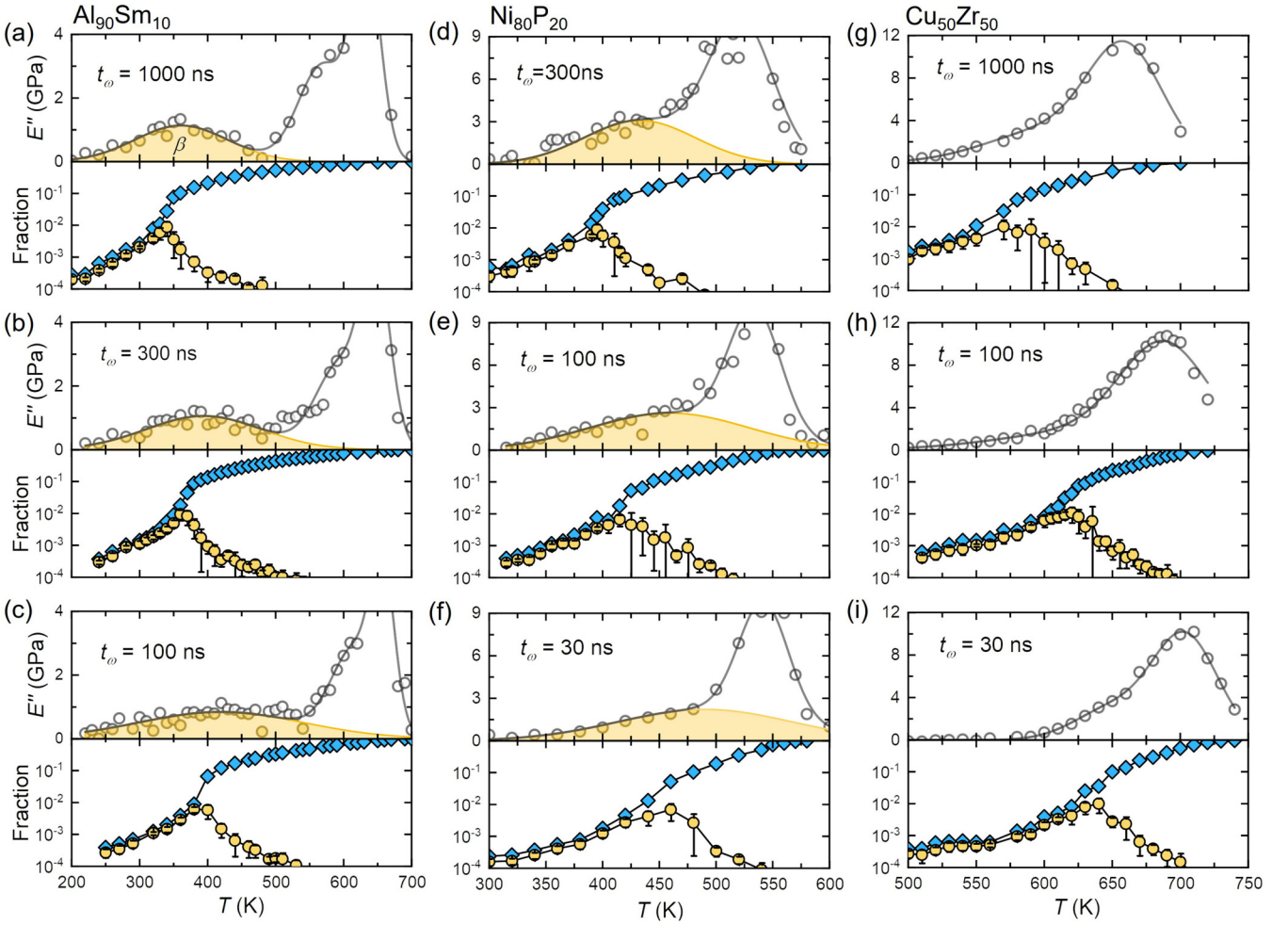
FIG. 2. Relaxation processes and percolation at different oscillation periods. (a)–(c) $Al_{90}Sm_{10}$; (d)–(f) $Ni_{80}P_{20}$; (g)–(i) $Cu_{50}Zr_{50}$. The β relaxation, when separable from the α relaxation, is indicated by the yellow shaded region in each plot.

is consistent with the observation of stringlike motions, as examples shown in the insets in Fig. 1(c).

To investigate the growth mechanism of clusters with temperature, we compute the correlation length $\xi = \sqrt{2 \sum_i R_{gi}^2 S_i^2 / \sum_i S_i^2}$ and relative size fraction S_{FLC}/N_{mobile} cluster [69]. Here, S_{FLC} is the size of the FLC, N_{mobile} is the number of mobile atoms, and R_{gi} is the radius of gyration for cluster size S_i.

Typically, as shown for an $Al_{90}Sm_{10}$ system in Fig. 3(c), correlation length ξ increases with the fraction P of mobile atoms and reaches a maximum near a critical fraction $P_c = 0.1$. Here, this maximum $\xi \sim 72$ Å at P_c is limited by the simulation box, and we have validated this in a large model in Fig. S10(f). In a thermodynamic limit ($V \to \infty$), it will diverge without a typical size. In addition, a power law relation $\xi \sim (P_c - P)^{-\nu}$ can be seen in the inset of Fig. 3(c) with $\nu = 0.89$ when P is near P_c, reinforcing the critical-like behavior for percolation [69,70].

As shown in Fig. 3(d), S_{FLC}/N_{mobile} increases monotonically with the fraction P of mobile atoms to total atoms. This indicates that the size of the FLC increases with other mobile clusters, and the mobile clusters are easily attached into the FLC. A sigmoidal-like rapid growth of S_{FLC}/N_{mobile} can be observed around $P_c \sim 0.1$, which is consistent with the

percolation. Figure S11 presents validation of this finding in other systems.

Hence, as shown in the inset of Fig. 3(d), the percolation occurs when about $P_c \sim 10\%$ of the atoms are mobile. We have reproduced this finding in other systems in Figs. S10 and S12. This value seems to be universal across different models of MGs.

In Fig. 4(a), we compared the temperature at $S_{FLC}/N_{mobile} = 0.5$ ($T_{0.5}$) and T_{SLC} for five systems with different oscillation periods. These data are collapsed onto a single line. It indicates that $S_{FLC}/N_{mobile} = 0.5$ is a status where other clusters are taken over (or merged) by the FLC rapidly. In addition, as shown in Fig. 4(b), we observed the percolation transition (T_{Pc}) of mobile clusters overlapped with β relaxation (T_β) in MG systems. This result indicates that β relaxation and the percolation of mobile clusters exhibit similar dynamics in terms of structural rearrangement.

III. DISCUSSION

We summarize in Fig. 5 for the temperature and time dependence of α, β relaxations and the percolation transition. The data for the percolation transition and the β relaxation are almost overlapped, and both gradually approach the α re-
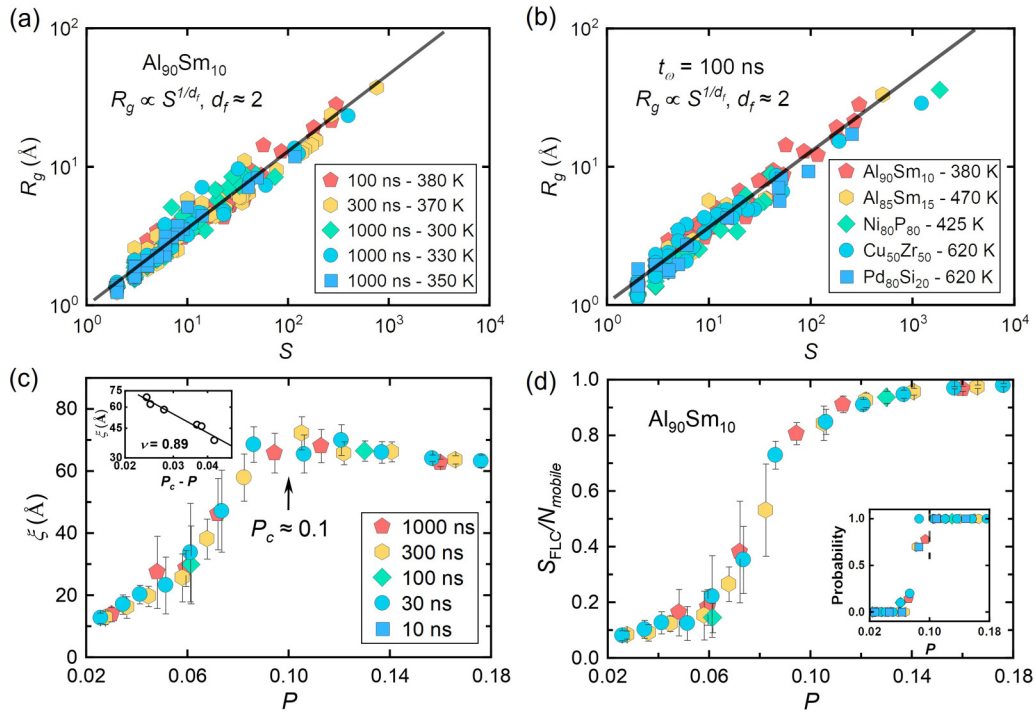
FIG. 3. Fractal structure and percolation of clusters. The radius of gyration R_g with size S of clusters for (a) $Al_{90}Sm_{10}$ glassy model with different oscillation periods t_ω and temperature; (b) $Al_{90}Sm_{10}$, $Al_{85}Sm_{15}$, $Ni_{80}P_{20}$, $Cu_{50}Zr_{50}$, and $Pd_{80}Si_{20}$ model MGs with an oscillation period $t_\omega = 100$ ns, at $T = T_{SLC}$. (c) Cluster correlation length ξ as a function of fraction P for $Al_{90}Sm_{10}$ models with different oscillation periods. The inset is $\xi \sim (P_c - P)^{-\nu}$ with $\nu = 0.89$. (d) Relative size fraction of atoms in FLC to the number of mobile atoms (S_{FLC}/N_{mobile}) as a function of fraction P of mobile atoms to total atoms (N_{mobile}/N_{total}) for $Al_{90}Sm_{10}$ models with different oscillation periods. The inset show the probability of finding a percolated (span) cluster.

laxation with increasing temperature. Eventually, they would merge with the α relaxation at the temperature. This implies that the observed percolation transition of mobile clusters is relevant to the origin of β relaxation in glasses.

Remarkably, Fig. 5 provides an answer to the long-standing question: Why do some glasses exhibit β relaxation as a pronounced peak [e.g., $Al_{90}Sm_{10}$ in Fig. 5(a)], a shoulder, or hump [$Ni_{80}P_{20}$ in Fig. 5(b)], while others as excess wings [e.g., $Cu_{50}Zr_{50}$ in Fig. 5(c)]?

Our results indicate that the early or late percolation of mobile clusters could be responsible for the behavior of β relaxation, either as a separated peak or excess wings. For example, the percolation of the FLC occurs at a low temperature in the $Al_{90}Sm_{10}$ MG (which is far away from the α relaxation), resulting in the β relaxation as a separate peak, whereas in the $Cu_{50}Zr_{50}$ MG, the percolation is very close to the α relaxation, and hence the excess wing forms with a large overlap to the α relaxation. In addition, as shown in Fig. S9(b), we have validated this scenario in a SiO_2 model; its percolation of the FLC is near the α relaxation. This implies that the β relaxation in SiO_2, if it exists, is coupled strongly with the α relaxation.

As the chemical compositions are crucial for the β relaxation [71–74]. Our work considers seven species of glass materials, which differ significantly in their chemical order. For example, when clusters percolated ($P = P_c$), approximately 0.1% of the atoms involved in clusters were Sm for $Al_{90}Sm_{10}$ glasses, while around 23.3% of the atoms involved in clusters were Zr for $Cu_{50}Zr_{50}$ glasses. This difference

suggests that at the present level of understanding based on percolation, the chemical orders are already "coarse grained." The chemical orders might have influence on the temperature of the percolation like in Fig. 5.

In a few studies, the β relaxation in MGs has been interpreted as resulting from the stringlike jumps of mobile atoms [22,24,28]. The excess wings are thought to be the less developed β relaxations, as atoms begin to break free from the cage relatively late, and are thus unable to develop the stringlike motions due to structural relaxation that occurs soon after, leading to cage collapse and global diffusion. This scenario is consistent with our findings based on percolation.

The interpretation based on percolation is more general than that of stringlike jumps [75]. Particularly in MGs, the stringlike motions can be considered as the basic events of β relaxation. They represent the detailed motion of these mobile atoms. The percolation of them leads to the microscopically detectable β relaxation, e.g., by mechanical spectra. For other types of glasses, the basic events might be different from stringlike motions (e.g., molecular rotation) [49]. The correlation between the β relaxation and percolation transition would still hold, where one might need to redefine the basic events or mobile clusters.

The percolation also offers a way for the correlation between mechanical properties and the β relaxation in MGs. For example, the percolated mobile clusters can be effective in dissipating the mechanical energy, leading to plas-
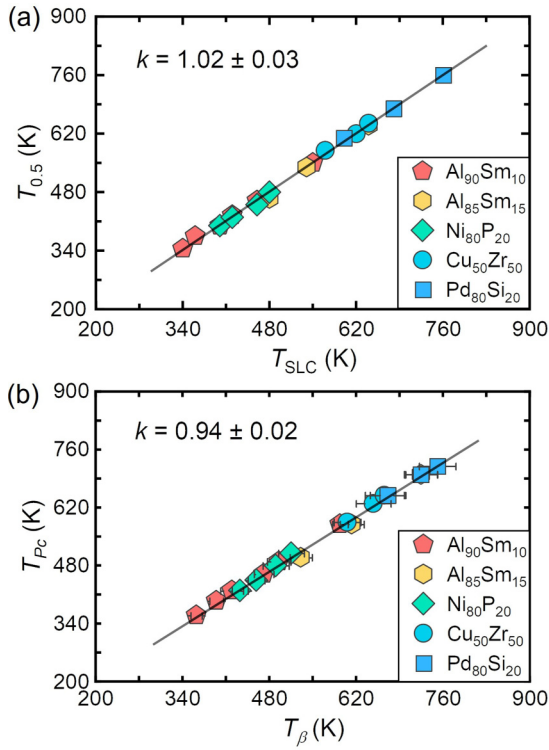
FIG. 4. Relation between percolation and β relaxation. (a) Comparison of the temperature at $S_{\max}/N_{\text{mobile}} = 0.5$ ($T_{0.5}$) and the critical temperature T_{SLC} for five systems with different oscillation periods t_ω. (b) Comparison of the temperature at P_c (T_{Pc}) and β relaxation temperature (T_β) shown in the patterns of DMS for all systems. In both (a) and (b) k is the slope of the linear fit (thin line).

tic deformation, stress relaxation, and slow hidden flow. In a stress-relaxation experiment [76], Wang *et al.* modeled the MG into the liquidlike zones and the elastic matrix. They calculated the fraction of a liquidlike zone at the onset of β relaxation, which is about $p_{\text{Liq}} \sim 0.08$ for a $\text{La}_{60}\text{Ni}_{15}\text{Al}_{25}$ MG. This value is consistent with our results that $P_c \sim 0.1$ universally.

Finally, we note that our percolation scenario is consistent with the predictions of the random first order transition theory. Stevenson and Wolynes [77] explored this theory, taking into account driving-force fluctuations and the diversity of reconfiguring shapes, and discovered an additional dynamical process that shares features of β relaxation. This process is governed by more ramified, stringlike, or percolationlike clusters of particles. Our simulation results align with this theoretical prediction and suggest that their theory is relevant to relaxation in realistic models.

IV. CONCLUSION

In summary, we have shown that mobility percolation transition follows the same dynamics of β relaxation in seven models of metallic glasses. The percolation transition universally occurs when the mobile atoms take up $\sim 10\%$, and the system spanning clusters are factual. The early or late percolation of mobile clusters has a direct consequence on behaviors of β relaxation, only if the percolation is far apart from α relaxation the β relaxation exhibits a clear peak. The excess wing is due to that the percolation occurs near the α relaxation. These results have been validated in seven model glasses. Looking forward, the concept of percolation provides a general mechanism for understanding the β relaxation in diverse disordered systems in a unified manner.
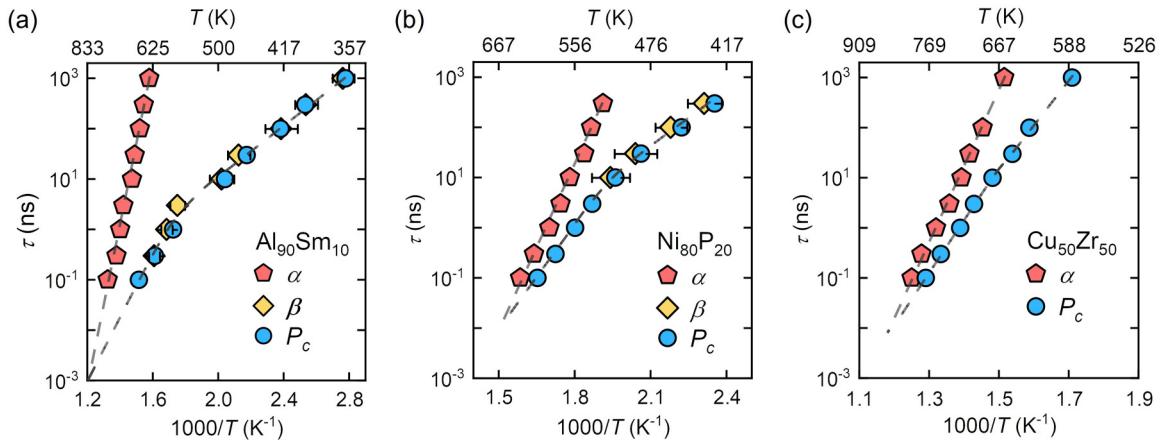

FIG. 5. Relaxation time map. The temperate-dependent relaxation time of α, β relaxations and the time of percolation of FLC for (a) $\text{Al}_{90}\text{Sm}_{10}$, (b) $\text{Ni}_{80}\text{P}_{20}$, and (c) $\text{Cu}_{50}\text{Zr}_{50}$ models.

ACKNOWLEDGMENTS

[1] K. L. Ngai, Relation between some secondary relaxations and the α relaxations in glass-forming materials according to the coupling model, J. Chem. Phys. **109**, 6982 (1998).

[2] K. L. Ngai, *Relaxation and Diffusion in Complex Systems* (Springer, New York, 2011).

[3] H. B. Yu, W. H. Wang, H. Y. Bai, and K. Samwer, The β-relaxation in metallic glasses, Natl. Sci. Rev. **1**, 429 (2014).

[4] W. H. Wang, Dynamic relaxations and relaxation-property relationships in metallic glasses, Prog. Mater. Sci. **106**, 100561 (2019).

[5] C. Chang, H. P. Zhang, R. Zhao, F. C. Li, P. Luo, M. Z. Li, and H. Y. Bai, Liquid-like atoms in dense-packed solid glasses, Nat. Mater. **21**, 1240 (2022).

[6] Q. Wang, S. T. Zhang, Y. Yang, Y. D. Dong, C. T. Liu, and J. Lu, Unusual fast secondary relaxation in metallic glass, Nat. Commun. **6**, 7876 (2015).

[7] P. Luo, Y. Z. Li, H. Y. Bai, P. Wen, and W. H. Wang, Memory Effect Manifested by a Boson Peak in Metallic Glass, Phys. Rev. Lett. **116**, 175901 (2016).

[8] Y. J. Duan, L. T. Zhang, T. Wada, H. Kato, E. Pineda, D. Crespo, J. M. Pelletier, and J. C. Qiao, Analysis of the anelastic deformation of high-entropy $Pd_{20}Pt_{20}Cu_{20}Ni_{20}P_{20}$ metallic glass under stress relaxation and recovery, J. Mater. Sci. Technol. **107**, 82 (2022).

[9] L. T. Zhang, Y. J. Duan, T. Wada, H. Kato, J. M. Pelletier, D. Crespo, E. Pineda, and J. C. Qiao, Dynamic mechanical relaxation behavior of $Zr_{35}Hf_{17.5}Ti_{5.5}Al_{12.5}Co_{7.5}Ni_{12}Cu_{10}$ high entropy bulk metallic glass, J. Mater. Sci. Technol. **83**, 248 (2021).

[10] Q. Yang, C. Q. Pei, H. B. Yu, and T. Feng, Metallic nanoglasses with promoted beta-relaxation and tensile plasticity, Nano Lett. **21**, 6051 (2021).

[11] H. B. Yu, X. Shen, Z. Wang, L. Gu, W. H. Wang, and H. Y. Bai, Tensile Plasticity in Metallic Glasses with Pronounced Beta Relaxations, Phys. Rev. Lett. **108**, 015504 (2012).

[12] Z. W. Wu, W. Kob, W. H. Wang, and L. Xu, Stretched and compressed exponentials in the relaxation dynamics of a metallic glass-forming melt, Nat. Commun. **9**, 5334 (2018).

[13] F. Spieckermann, D. Sopu, V. Soprunyuk, M. B. Kerber, J. Bednarcik, A. Schokel, A. Rezvan, S. Ketov, B. Sarac, E. Schafler, and J. Eckert, Structure-dynamics relationships in cryogenically deformed bulk metallic glass, Nat. Commun. **13**, 127 (2022).

[14] H. Jiang, J. Xu, Q. Zhang, Q. Yu, L. Shen, M. Liu, Y. Sun, C. Cao, D. Su, H. Bai, S. Meng, B. Sun, L. Gu, and W. Wang, Direct observation of atomic-level fractal structure in a metallic glass membrane, Sci. Bull. **66**, 1312 (2021).

[15] J. Ding, L. Li, N. Wang, L. Tian, M. Asta, R. O. Ritchie, and T. Egami, Universal nature of the saddle states of structural excitations in metallic glasses, Mater. Today Phys. **17**, 100359 (2021).

[16] Y. C. Hu, Y. W. Li, Y. Yang, P. F. Guan, H. Y. Bai, and W. H. Wang, Configuration correlation governs slow dynamics of supercooled metallic liquids, Proc. Natl. Acad. Sci. USA **115**, 6375 (2018).

[17] Z. Zhang, J. Ding, and E. Ma, Shear transformations in metallic glasses without excessive and predefinable defects, Proc. Natl. Acad. Sci. USA **119**, e2213941119 (2022).

[18] I. Binkowski, G. P. Shrivastav, J. Horbach, S. V. Divinski, and G. Wilde, Shear band relaxation in a deformed bulk metallic glass, Acta Mater. **109**, 330 (2016).

[19] Y. H. Liu, T. Fujita, D. P. Aji, M. Matsuura, and M. W. Chen, Structural origins of Johari-Goldstein relaxation in a metallic glass, Nat. Commun. **5**, 3238 (2014).

[20] Y. Sun, S. X. Peng, Q. Yang, F. Zhang, M. H. Yang, C. Z. Wang, K. M. Ho, and H. B. Yu, Predicting Complex Relaxation Processes in Metallic Glass, Phys. Rev. Lett. **123**, 105701 (2019).

[21] Z. Y. Zhou, Q. Chen, Y. Sun, and H. B. Yu, Unveiling correlation between α_2 relaxation and yielding behavior in metallic glasses, Phys. Rev. B **103**, 094117 (2021).

[22] H. B. Yu, M. H. Yang, Y. Sun, F. Zhang, J. B. Liu, C. Z. Wang, K. M. Ho, R. Richert, and K. Samwer, Fundamental link between beta relaxation, excess wings, and cage-breaking in metallic glasses, J. Phys. Chem. Lett. **9**, 5877 (2018).

[23] H. B. Yu, Y. Luo, and K. Samwer, Ultrastable metallic glass, Adv. Mater. **25**, 5904 (2013).

[24] H. B. Yu, R. Richert, and K. Samwer, Structural rearrangements governing Johari-Goldstein relaxations in metallic glasses, Sci. Adv. **3**, e1701577 (2017).

[25] H. W. Bi, A. Inoue, F. F. Han, Y. Han, F. L. Kong, S. L. Zhu, E. Shalaan, F. Al-Marzouki, and A. L. Greer, Novel deformation-induced polymorphic crystallization and softening of Al-based amorphous alloys, Acta Mater. **147**, 90 (2018).

[26] S. Sun and P. Guan, The critical model size for simulating the structure-dynamics correlation in bulk metallic glasses, Sci. China Mater. **64**, 1545 (2021).

[27] Q. Yang, S. X. Peng, Z. Wang, and H. B. Yu, Shadow glass transition as a thermodynamic signature of β relaxation in hyper-quenched metallic glasses, Natl. Sci. Rev. **7**, 1896 (2020).

[28] Z. Y. Zhou, Y. Sun, L. Gao, Y. J. Wang, and H.-B. Yu, Fundamental links between shear transformation, β relaxation, and string-like motion in metallic glasses, Acta Mater. **246**, 118701 (2023).

[29] H. Yu, W.-H. Wang, and K. Samwer, The β relaxation in metallic glasses: An overview, Mater. Today **16**, 183 (2013).

[30] H. B. Yu, M. Tylinski, A. Guiseppi-Elie, M. D. Ediger, and R. Richert, Suppression of Beta Relaxation in Vapor-Deposited Ultrastable Glasses, Phys. Rev. Lett. **115**, 185501 (2015).

[31] B. Guiselin, C. Scalliet, and L. Berthier, Microscopic origin of excess wings in relaxation spectra of supercooled liquids, Nat. Phys. **18**, 468 (2022).

[32] F. Zhu, H. K. Nguyen, S. X. Song, D. P. Aji, A. Hirata, H. Wang, K. Nakajima, and M. W. Chen, Intrinsic correlation between beta-relaxation and spatial heterogeneity in a metallic glass, Nat. Commun. **7**, 11516 (2016).

[33] M. T. Cicerone, Q. Zhong, and M. Tyagi, Picosecond Dynamic Heterogeneity, Hopping, and Johari-Goldstein Relaxation in Glass-Forming Liquids, Phys. Rev. Lett. **113**, 117801 (2014).

[34] K. L. Ngai, L. M. Wang, and H. B. Yu, Relating Ultrastable Glass Formation to Enhanced Surface Diffusion via the Johari-Goldstein beta-Relaxation in Molecular Glasses, J. Phys. Chem. Lett. **8**, 2739 (2017).

[35] J. Mattsson, R. Bergman, P. Jacobsson, and L. Börjesson, Chain-Length-Dependent Relaxation Scenarios in an Oligomeric Glass-Forming System: From Merged to Well-Separated A and B Loss Peaks, Phys. Rev. Lett. **90**, 075702 (2003).

[36] S. Napolitano, E. Glynos, and N. B. Tito, Glass transition of polymers in bulk, confined geometries, and near interfaces, Rep. Prog. Phys. **80**, 036602 (2017).

[37] M. Paluch, Z. Wojnarowska, and S. Hensel-Bielowka, Heterogeneous Dynamics of Prototypical Ionic Glass Ckn Monitored by Physical Aging, Phys. Rev. Lett. **110**, 015702 (2013).

[38] S. He, Y. Li, L. Liu, Y. Jiang, J. Feng, W. Zhu, J. Zhang, Z. Dong, Y. Deng, J. Luo, W. Zhang, and G. Chen, Semiconductor glass with superior flexibility and high room temperature thermoelectric performance, Sci. Adv. **6**, eaaz8423 (2020).

[39] W. H. Wang, The elastic properties, elastic models and elastic perspectives of metallic glasses, Prog. Mater. Sci. **57**, 487 (2012).

[40] J. C. Qiao, Q. Wang, J. M. Pelletier, H. Kato, R. Casalini, D. Crespo, E. Pineda, Y. Yao, and Y. Yang, Structural heterogeneities and mechanical behavior of amorphous alloys, Prog. Mater. Sci. **104**, 250 (2019).

[41] M. Bhattacharya, Polymer nanocomposites-a comparison between carbon nanotubes, graphene, and clay as nanofillers, Materials **9**, 262 (2016).

[42] S. X. Peng, Y. Cheng, J. Pries, S. Wei, H. B. Yu, and M. Wuttig, Uncovering β-relaxations in amorphous phase-change materials, Sci. Adv. **6**, eaay6726 (2020).

[43] S. Baghel, H. Cathcart, and N. J. O'Reilly, Polymeric amorphous solid dispersions: A review of amorphization, crystallization, stabilization, solid-state characterization, and aqueous solubilization of biopharmaceutical classification system class II drugs, J. Pharm. Sci. **105**, 2527 (2016).

[44] H. B. Yu, R. Richert, R. Maass, and K. Samwer, Strain induced fragility transition in metallic glass, Nat. Commun. **6**, 7179 (2015).

[45] H. B. Yu, R. Richert, R. Maass, and K. Samwer, Unified Criterion for Temperature-Induced and Strain-Driven Glass Transitions in Metallic Glass, Phys. Rev. Lett. **115**, 135701 (2015).

[46] K. Tao, J. C. Qiao, Q. F. He, K. K. Song, and Y. Yang, Revealing the structural heterogeneity of metallic glass: Mechanical spectroscopy and nanoindentation experiments, Int. J. Mech. Sci. **201**, 106469 (2021).

[47] C. P. Royall and S. R. Williams, The role of local structure in dynamical arrest, Phys. Rep. **560**, 1 (2015).

[48] G. P. Johari and M. Goldstein, Viscous liquids and the glass transition. II. Secondary relaxations in glasses of rigid molecules, J. Chem. Phys. **53**, 2372 (1970).

[49] G. P. Johari, Glass-transition and secondary relaxations in molecular liquids and crystals, Ann. N. Y. Acad. Sci. **279**, 117 (1976).

[50] G. P. Johari, Source of JG-relaxation in the entropy of glass, J. Phys. Chem. B **123**, 3010 (2019).

[51] J. S. Harmon, M. D. Demetriou, W. L. Johnson, and K. Samwer, Anelastic to Plastic Transition in Metallic Glass-Forming Liquids, Phys. Rev. Lett. **99**, 135502 (2007).

[52] X. D. Wang, J. Zhang, T. D. Xu, Q. Yu, Q. P. Cao, D. X. Zhang, and J. Z. Jiang, Structural signature of beta-relaxation in la-based metallic glasses, J. Phys. Chem. Lett. **9**, 4308 (2018).

[53] A. Heuer, Properties of a Glass-Forming System as Derived from Its Potential Energy Landscape, Phys. Rev. Lett. **78**, 4051 (1997).

[54] See Supplemental Material at http://link.aps.org/supplemental/10.1103/PhysRevB.108.014201 for details of simulations and percolation cluster analysis, which includes Refs. [55–66].

[55] S. Munetoh, T. Motooka, K. Moriguchi, and A. Shintani, Interatomic potential for Si–O systems using Tersoff parameterization, Comput. Mater. Sci. **39**, 334 (2007).

[56] M. I. Mendelev, M. J. Kramer, R. T. Ott, D. J. Sordelet, D. Yagodin, and P. Popel, Development of suitable interatomic potentials for simulation of liquid and amorphous Cu–Zr alloys, Philos. Mag. **89**, 967 (2009).

[57] A. Stukowski, Visualization and analysis of atomistic simulation data with OVITO–the open visualization tool, Model. Simul. Mater. Sci. Eng. **18**, 015012 (2010).

[58] W. M. Brown, P. Wang, S. J. Plimpton, and A. N. Tharrington, Implementing molecular dynamics on hybrid high performance computers–short range forces, Comput. Phys. Commun. **182**, 898 (2011).

[59] W. M. Brown, A. Kohlmeyer, S. J. Plimpton, and A. N. Tharrington, Implementing molecular dynamics on hybrid high performance computers–Particle–particle particle-mesh, Comput. Phys. Commun. **183**, 449 (2012).

[60] H. W. Sheng, E. Ma, and M. J. Kramer, Relating dynamic properties to atomic structure in metallic glasses, JOM **64**, 856 (2012).

[61] W. M. Brown and M. Yamada, Implementing molecular dynamics on hybrid high performance computers—Three-body potentials, Comput. Phys. Commun. **184**, 2785 (2013).

[62] H. B. Yu and K. Samwer, Atomic mechanism of internal friction in a model metallic glass, Phys. Rev. B **90**, 144201 (2014).

[63] M. I. Mendelev, F. Zhang, Z. Ye, Y. Sun, M. C. Nguyen, S. R. Wilson, C. Z. Wang, and K. M. Ho, Development of interatomic potentials appropriate for simulation of devitrification of $Al_{90}Sm_{10}$ alloy, Modell. Simul. Mater. Sci. Eng. **23**, 045013 (2015).

[64] J. Ding, M. Asta, and R. O. Ritchie, On the question of fractal packing structure in metallic glasses, Proc. Natl. Acad. Sci. USA **114**, 8458 (2017).

[65] T. D. Nguyen, GPU-accelerated Tersoff potentials for massively parallel molecular dynamics simulations, Comput. Phys. Commun. **212**, 113 (2017).

[66] A. P. Thompson, H. M. Aktulga, R. Berger, D. S. Bolintineanu, W. M. Brown, P. S. Crozier, P. J. in 't Veld, A. Kohlmeyer, S. G. Moore, T. D. Nguyen, R. Shan, M. J. Stevens, J. Tranchida, C. Trott, and S. J. Plimpton, LAMMPS - a flexible simulation tool for particle-based materials modeling at the atomic, meso, and continuum scales, Comput. Phys. Commun. **271**, 108171 (2022).

[67] H. B. Yu, R. Richert, and K. Samwer, Correlation between viscoelastic moduli and atomic rearrangements in metallic glasses, J. Phys. Chem. Lett. **7**, 3747 (2016).

[68] A. Ghosh, Z. Budrikis, V. Chikkadi, A. L. Sellerio, S. Zapperi, and P. Schall, Direct Observation of Percolation in the Yielding Transition of Colloidal Glasses, Phys. Rev. Lett. **118**, 148001 (2017).

[69] D. Stauffer and A. Aharony, *Introduction to Percolation Theory* (Taylor & Francis, London, 1994).

[70] M. D. Rintoul and S. Torquato, Precise determination of the critical threshold and exponents in a three-dimensional continuum percolation model, J. Phys. A: Math. Gen. **30**, L585 (1997).

[71] Y.-C. Hu, W. Jin, J. Schroers, M. D. Shattuck, and C. S. O'Hern, Glass-forming ability of binary Lennard-Jones systems, Phys. Rev. Mater. **6**, 075601 (2022).

[72] Y. C. Hu and H. Tanaka, Revealing the role of liquid preordering in crystallisation of supercooled liquids, Nat. Commun. **13**, 4519 (2022).

[73] Y.-C. Hu and H. Tanaka, Physical origin of glass formation from multicomponent systems, Sci. Adv. **6**, eabd2928 (2020).

[74] Y.-C. Hu, J. Schroers, M. D. Shattuck, and C. S. O'Hern, Tuning the glass-forming ability of metallic glasses through energetic frustration, Phys. Rev. Mater. **3**, 085602 (2019).

[75] Z. Wang and W. H. Wang, Flow units as dynamic defects in metallic glassy materials, Natl. Sci. Rev. **6**, 304 (2019).

[76] Z. Wang, B. A. Sun, H. Y. Bai, and W. H. Wang, Evolution of hidden localized flow during glass-to-liquid transition in metallic glass, Nat. Commun. **5**, 5823 (2014).

[77] J. D. Stevenson and P. G. Wolynes, A universal origin for secondary relaxations in supercooled liquids and structural glasses, Nat. Phys. **6**, 62 (2010).